Photodissociation of CO_2^- in water clusters via Renner-Teller and conical interactions

Terefe Habteyes, Luis Velarde, and Andrei Sanov
Department of Chemistry, University of Arizona, 1306 E. University Boulevard, Tucson, Arizona 85721-0041

(Received 24 January 2007; accepted 26 February 2007; published online 16 April 2007)

The photochemistry of mass selected $CO_2^-(H_2O)_m$, $m=2-40$ cluster anions is investigated using 266 nm photofragment spectroscopy and theoretical calculations. Similar to the previous 355 nm experiment [Habteyes *et al.*, Chem. Phys. Lett. **424**, 268 (2006)], the fragmentation at 266 nm yields two types of anionic products: $O^-(H_2O)_{m-k}$ (core-dissociation products) and $CO_2^-(H_2O)_{m-k}$ (solvent-evaporation products). Despite the same product types, different electronic transitions and dissociation mechanisms are implicated at 355 and 266 nm. The 355 nm dissociation is initiated by excitation to the first excited electronic state of the CO_2^- cluster core, the $1\ ^2B_1(^2A'')$ state, and proceeds via a glancing Renner-Teller intersection with the ground electronic state at a linear geometry. The 266 nm dissociation involves the second excited electronic state of CO_2^-, the $2\ ^2A_1(^2A')$ state, which exhibits a conical intersection with the $3\ ^2B_2(A')$ state at a bent geometry. The asymptotic O^- based products are believed to be formed via this $3\ ^2B_2(A')$ state. By analyzing the fragmentation results, the bond dissociation energy of CO_2^- to O^-+CO in hydrated clusters ($m \geqslant 20$) is estimated as 2.49 eV, compared to 3.46 eV for bare CO_2^-. The enthalpy of evaporation of one water molecule from asymptotically large $CO_2^-(H_2O)_m$ clusters is determined to be 0.466 ± 0.001 eV (45.0 ± 0.1 kJ/mol). This result compares very favorably with the heat of evaporation of bulk water, 0.456 eV (43.98 kJ/mol). © *2007 American Institute of Physics*.
[DOI: 10.1063/1.2717932]

I. INTRODUCTION

The metastable anion of CO_2 has been observed in numerous processes. Examples include CO_2^+ impact on metals;[1] electron impact on formic acid;[2] γ-ray irradiation of sodium formate crystals;[3] CO_2 adsorption on UV-irradiated MgO surface;[4] CO_2 reactions with negative ions;[5] pulse radiolysis of aqueous solutions of carbon monoxide, carbon dioxide, sodium formate, formic acid, sodium bicarbonate, and aliphatic acids;[6,7] and electron collisions with cyclic anhydrides.[8] Short-lived CO_2^- resonances are also implicated in electron scattering on neutral CO_2.[9–11] The lifetime of relaxed CO_2^- against autodetachment is estimated at 60–90 μs,[8,12] which is rather long on the time scale of most gas-phase experiments. The autodetachment can be further slowed or even suppressed by the effect of homogeneous[13] or heterogeneous[14] solvation.

The homogeneous solvation in the $(CO_2)_n^-$ clusters is known to affect the constitution of the core anion, which switches between the CO_2^- and $O_2CCO_2^-$ forms depending on the cluster size.[15–17] In the hydrated cluster anions of carbon dioxide, $[CO_2(H_2O)_m]^-$, the extra electron has been shown to localize on the CO_2^- core[18] despite the negative adiabatic electron affinity of CO_2.[12] Hence, these clusters are properly described as $CO_2^-(H_2O)_m$. In the absence of CO_2, the vertical detachment energies (VDEs) of the hydrated electron clusters are rather modest, varying from only 45 ± 5 meV for $(H_2O)_2^-$ to 0.79–1.92 eV for $(H_2O)_m^-$ in the $m=11-69$ range.[19–23] These values are consistent with a delocalized nature of the hydrated electron within the network of water molecules. "Doping" the cluster with CO_2 increases the detachment energies quite dramatically, i.e., to 1.96–3.46 eV for $CO_2^-(H_2O)_m$, $m=1-5$.[18,24] These values reflect strong hydration interactions with a localized anionic core. Consistent with these energetics, a mixture of CO_2 and $(H_2O)_m^-$ converts completely to the $CO_2^-(H_2O)_m$ cluster form within 0.5 s.[25]

Past photoelectron imaging results for $CO_2^-(H_2O)_m$, $m=1-6$ hinted at the role of excited anionic states of these clusters, which increases gradually with m.[18] While electron detachment is the dominant photodestruction pathway in the small cluster-size range, the excited-state contribution to the photodetachment comes in the form of poorly structured autodetachment signal. However, with increasing hydration, the electron removal becomes progressively less favorable energetically, yielding stage to anionic rearrangements. Some aspects of this reactivity were revealed in our recent 355 nm photofragmentation study of the $CO_2^-(H_2O)_m$, $m=3-20$ clusters.[26] The results illuminated the important role of the solvent (H_2O in particular) in controlling the excited-state decay channels. As the electron photodetachment is gradually turned off with increasing cluster size, it is replaced by the anionic fragmentation involving hydration-stabilized excited states of CO_2^-. In the smaller $CO_2^-(H_2O)_m$ clusters ($m \leqslant 7$), the core-dissociation products, $O^-(H_2O)_{m-k}$, dominate the 355 nm fragmentation pathways. As m increases, the solvent-evaporation pathways, $CO_2^-(H_2O)_{m-k}$, attributed to caging of the nascent O^-+CO photofragments, gradually take precedence. It was also shown that adding a second CO_2 to the parent cluster with $m=4-6$ opens another channel

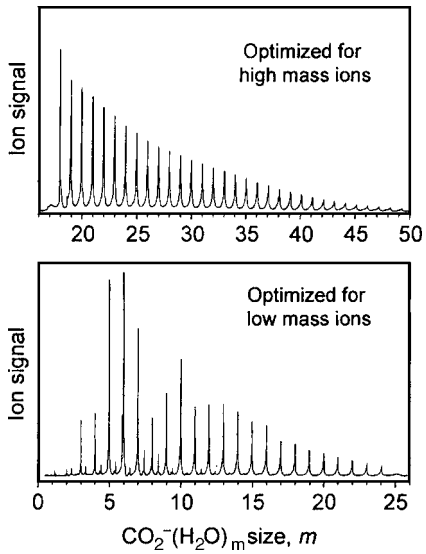

FIG. 1. Parent-ion mass spectra optimized for high mass (top) and low mass (bottom) ions.

involving an intracluster ion-molecule reaction of the nascent O^- with the second CO_2, yielding CO_3^- based products.[27]

In this work we report the photofragmentation of $CO_2^-(H_2O)_m$ with m up to 40, using 266 nm radiation. At this wavelength, the fragmentation is believed to proceed via a different, compared to 355 nm, set of excited states. Aided by *ab initio* calculations, the experiments investigate the role of the solvent in mediating the reactivity.

II. EXPERIMENTAL APPARATUS

The experiments are carried out using the anion spectrometer described in detail elsewhere.[27] In brief, the apparatus consists of (1) a cluster-ion source, (2) a tandem time-of-flight (TOF) mass spectrometer,[28] and (3) a velocity-map[29] imaging[30] assembly for the detection of photoelectrons. Only the first two components are employed in the present study.

The $CO_2^-(H_2O)_m$ cluster anions are prepared by expansion of undried CO_2 at a stagnation pressure of 2 atm through a pulsed supersonic nozzle (General Valve Series 99, 0.8 mm nozzle diameter) into a vacuum chamber with a base pressure of 2×10^{-7} Torr. Carbon dioxide tank impurities and trace amounts of water within the gas delivery lines serve as the source of H_2O. A continuous 1 keV electron beam crosses the supersonic expansion several millimeters from the valve orifice. The cluster anions are formed by secondary-electron attachment to neutral clusters.[28] A transverse, pulsed electric field (~1 kV/15 cm) is applied 18 cm downstream from the supersonic valve, extracting the anions into the 2.3 m long flight tube of a Wiley-McLaren TOF mass spectrometer, where they are further accelerated to a beam energy of about 3 keV.

After passing through a set of ion-optical components,[31] the ions are brought to a temporal and spatial focus in the detection region of the instrument (base pressure of 5×10^{-9} Torr). They are detected with TOF resolution using an in-line microchannel plate (MCP) detector (Burle, Inc.) mounted at the end of the flight tube. Figure 1 shows two representative mass spectra of the $CO_2^-(H_2O)_m$ parent ions corresponding to different ion source conditions, optimized for the small and large clusters, respectively.

The mass-selected cluster anions of interest are interrogated using an appropriately timed pulsed laser beam. The ionic photofragments are then analyzed using a single-field reflectron mass spectrometer, which separates the parent and assorted fragment ions according to their masses. The reflectron is tilted at 2.5° with respect to the primary TOF axis, deflecting the ions by 175° relative to the incoming beam. The reflected ions are detected by an off-axis MCP detector (Burle, Inc.) mounted at the spatial focus of the reflectron.

The fourth harmonic of a Nd:YAG (yttrium aluminum garnet) laser (Spectra Physics Lab 130-50) is used in this experiment, giving 266 nm, 8 mJ pulses at a repetition rate of 50 Hz. The laser beam is brought to a 5 mm diameter inside the vacuum chamber. The photofragment signals are typically averaged for 512 experimental cycles, transferred to a computer and analyzed as described elsewhere.[28,32,33]

III. EXPERIMENTAL RESULTS

The fragmentation measurements were performed at 266 nm on $CO_2^-(H_2O)_m$ cluster anions with m up to 40. The photofragment-ion mass spectra for $m=2-25$ are shown in Fig. 2. The results for the larger clusters (up to $m=40$) are included in the analysis, but the individual fragment mass spectra are not shown to save space. All spectra in Fig. 2 are normalized to the same (arbitrary) maximum intensity, not representative of the absolute cross sections. In particular, the low signal-to-noise ratio apparent in the $m=2$ spectrum reflects the weak intensity of the corresponding parent ion (as seen in Fig. 1), as well as the prevalence of the photodetachment.

Similar to our previous 355 nm study,[26] the observed fragmentation pattern can be summarized in terms of two types of anionic products: (1) $O^-(H_2O)_{m-k}$ and (2) $CO_2^-(H_2O)_{m-k}$, where k is the number of water molecules lost in the process. Type (1) fragments imply the dissociation of the CO_2^- core within the cluster. Therefore, the fragmentation pathways described by

$$CO_2^-(H_2O)_m + h\nu \rightarrow O^-(H_2O)_{m-k} + kH_2O \quad (1)$$

are collectively referred to as the core-dissociation channel. This channel is observed for parent clusters as small as $m=2$.

In the second type of fragmentation pathways,

$$CO_2^-(H_2O)_m + h\nu \rightarrow CO_2^-(H_2O)_{m-k} + kH_2O, \quad (2)$$

the core anion remains intact and the corresponding processes are referred to collectively as the solvent-evaporation channel. As the parent cluster size is increased, channel (2) opens at $m=9$ (compared to $m=6$ at 355 nm).[26] The m dependent branching between channels (1) and (2) at 266 and 355 nm is summarized in Fig. 3.

The average loss of water molecules, $\langle k\rangle$, in different fragmentation channels is summarized in Fig. 4. For channel (1) at 266 nm, $\langle k\rangle$ varies between 0.5 and 4.7 depending on m, while channel (2) involves the average loss of between

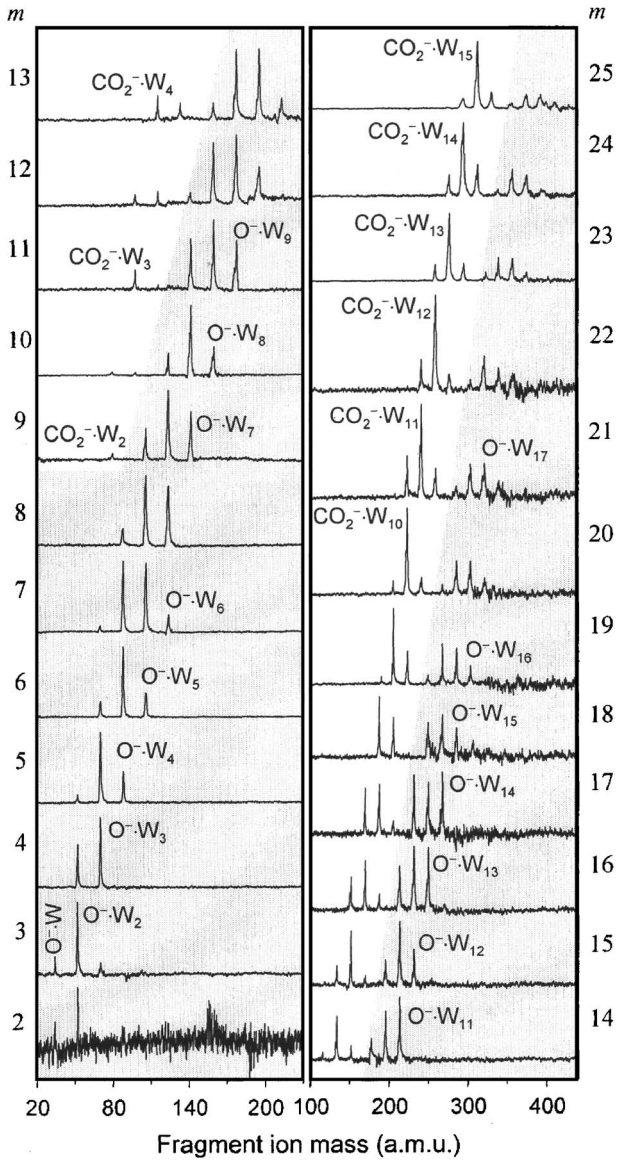

FIG. 2. Photofragment-ion mass spectra for the $CO_2^-(H_2O)_m$ cluster anions at 266 nm. The numbers on the right and on the left indicate the number of water molecules, m, in the parent clusters. For clarity, the peaks assigned to the core-dissociation fragments, $O^-\cdot W_{m-k}$, are shown against the gray background $W \equiv H_2O$.

7.0 and 10.0 water molecules. In both channels and at both 355 and 266 nm, $\langle k \rangle$ increases with m for small parent clusters, eventually approaching an asymptotic limit. Assuming that the asymptotic value of $\langle k \rangle = 10.0$ in channel (2) at 266 nm accounts for the dissipation of the entire photon energy, the average enthalpy of evaporation of one H_2O in the large-cluster limit is determined as 0.466 ± 0.001 eV (45.0 ± 0.1 kJ/mol), in agreement with our previous report.[26]

To shed light on the 266 and 355 nm fragmentation mechanisms, we compared the corresponding dissociation cross sections using the integrated intensities of all photofragments normalized to the laser power and parent-ion intensity. For small parent clusters ($m=3$), the 266 nm dissociation cross section was found to exceed that at 355 nm by more than an order of magnitude. However, the ratio of the two decreases with m and for $m \approx 10$ the two cross sections become approximately similar.

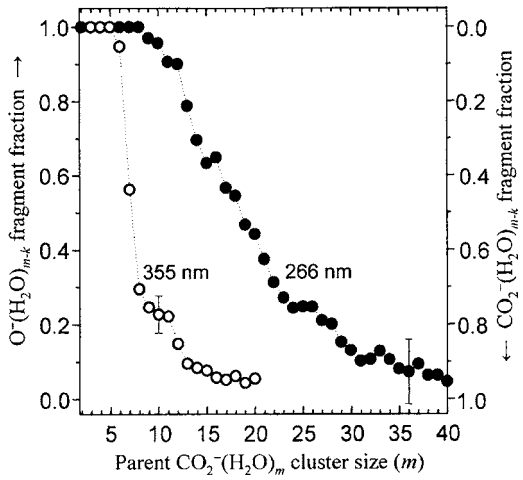

FIG. 3. Fractions of the $O^-(H_2O)_{m-k}$ and $CO_2^-(H_2O)_{m-k}$ products observed in the photofragmentation of $CO_2^-(H_2O)_m$ at 355 nm (open circles) and 266 nm (solid circles), plotted as functions of the parent cluster size.

IV. THEORETICAL ANALYSIS AND DISCUSSION

A. Trapping of the CO_2^-

CO_2 presents a well-known case of a molecule with negative adiabatic electron affinity, yet corresponding to markedly positive vertical detachment energy of its negative ion. The CO_2^- equilibrium corresponds to a bent geometry ($\angle OCO \approx 135°$) and even though the neutral ground state (at $\angle OCO = 180°$) lies lower in energy, the neutral potential energy at the bent anion geometry exceeds that of the anion.[34]

The most obvious effect of hydration is the lowering of

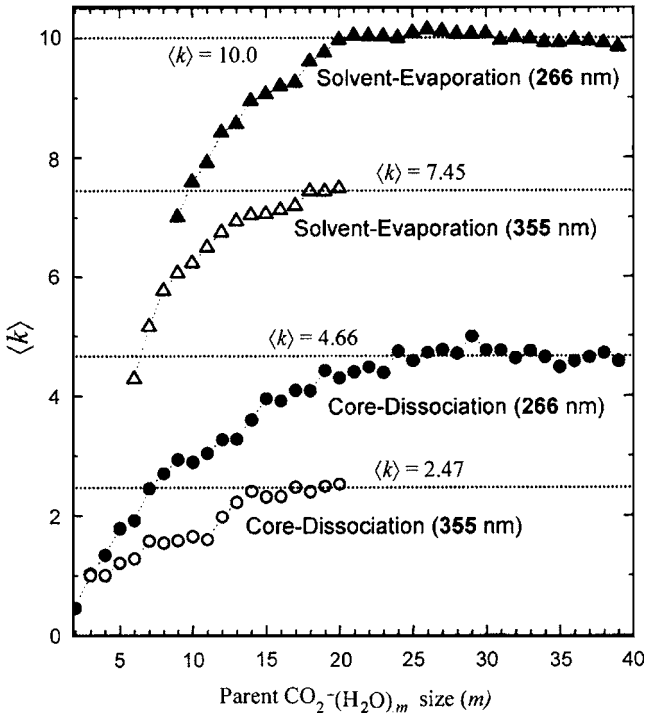

FIG. 4. Average numbers of water molecules evaporated in the core-dissociation and solvent-evaporation channels at 355 and 266 nm, as labeled. The dotted horizontal lines indicate the asymptotic values of $\langle k \rangle$ for each process.

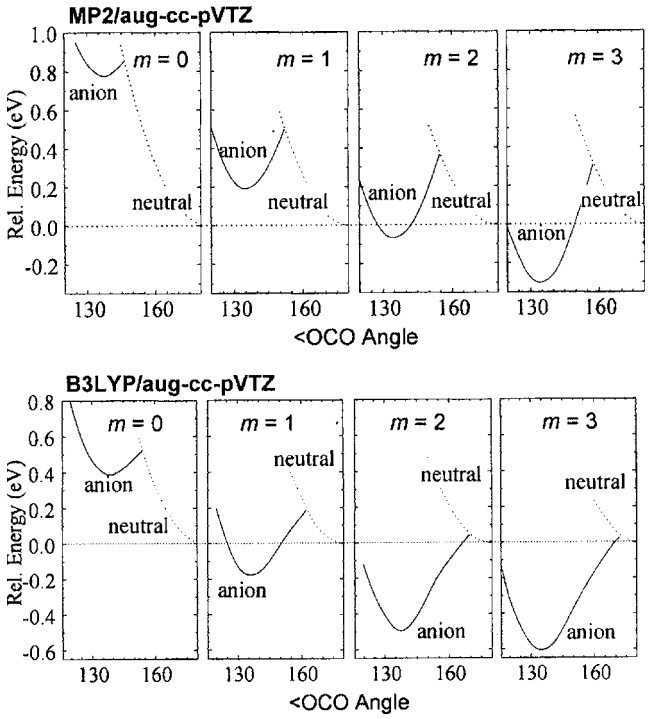

FIG. 5. The OCO bending angle dependence of the relative potential energies of $CO_2^-(H_2O)_m$ vs $CO_2(H_2O)_m$, $m=0$, 1, 2, and 3, calculated using the *ab initio* and density-functional methods (top and bottom panels, respectively), as described in the text.

the equilibrium energy of metastable CO_2^- with respect to that of neutral CO_2. In addition, as we discuss below, the hydration increases the height of the barrier, impeding the anion tunneling into the region of the coordinate space where rapid autodetachment will occur, effectively trapping the anion in its equilibrium.

The bending potential energy curves of CO_2^- and CO_2, calculated as explained later in this section, are shown in Fig. 5 (top and bottom, $m=0$). The crossing of the anion and neutral potentials results in a barrier separating the metastable anion equilibrium from the autodetachment continuum. The barrier plays a critical role in determining the anion stability. Referring to it briefly as the autodetachment barrier, we explore how its height is affected by the hydration in the $CO_2^-(H_2O)_m$ cluster anions.

Quantitative modeling of the anionic states of carbon dioxide requires highly correlated methods and large basis sets including very diffuse functions,[35] which are rather challenging to apply to relatively large systems, such as cluster anions. However, the approximate effect of stepwise hydration on the anion stability can be estimated using computationally inexpensive methods and basis sets. We calculated[36] the bending potential energy curves for the anion and neutral species of interest using the following procedure.

First, the geometries of $CO_2^-(H_2O)_m$, $m=0-3$ and the corresponding neutral clusters were optimized using MP2/6-31+G* calculations. The global-minimum geometries of the $CO_2^-(H_2O)_m$, $m=0-3$ cluster anions were reported previously.[18] The geometries of the neutral species were optimized starting from the corresponding anion equilibria. The resulting structures of the $m=1,2$ neutral clusters compare favorably with the previous experimental[37–42] and theoretical[25,43–46] results. There are no experimental data available for the $m=3$ neutral structure, but our optimized geometry agrees with the previously reported B3LYP result.[25]

Then, the OCO bending angle was scanned in 5°–10° increments, starting from the corresponding anion and neutral equilibrium geometries. At each fixed bending angle, all other cluster degrees of freedom were relaxed. The resulting partially relaxed geometries were used in single-point MP2 and B3LYP calculations with Dunning's aug-cc-pVTZ basis set to determine the corresponding potential energy values. The resulting energy curves are shown in Fig. 5, where the neutral energy minima are set arbitrarily to zero. The limitations of these calculations will be emphasized shortly, but first we focus on the insight that they do provide.

The $m=0$ case corresponds to bare CO_2^-. The *ab initio* curves in the top panel of Fig. 5 place the CO_2^- equilibrium 0.72 eV above the corresponding neutral minimum (including the zero-point energies). This result compares quite favorably with the −0.67 eV adiabatic electron affinity of CO_2 calculated by Gutsev *et al.*[34] at a higher level of theory [CCSD(T)/6-311+G(3*df*)]. For $m=1$, our *ab initio* calculations find the anion minimum 0.16 eV above the neutral equilibrium. The addition of the second water molecule ($m=2$) effectively evens the anion and neutral equilibrium potential energies (see Fig. 5, top), while a third H_2O ($m=3$) makes the anion adiabatically more stable than the corresponding neutral cluster by 0.18 eV.

Although the overall trend remains the same, the quantitative results of the density-functional (B3LYP) calculations differ significantly from the MP2 predictions (the top versus bottom parts of Fig. 5). For example, the negative electron affinity (−0.16 eV) for $m=1$ obtained using MP2 is in contrast to the positive electron affinity (0.17 eV) obtained using the B3LYP method.[25]

On the other hand, the adiabatic electron affinity of bare CO_2 calculated using the MP2 method (−0.72 eV) is in better agreement with the experimental value (−0.60±0.2 eV) (Ref. 12) than the B3LYP prediction (−0.34 eV). At the same time, the VDE of CO_2^- calculated using B3LYP (1.19 eV) is closer to the experiment (1.4 eV) (Ref. 47) than the MP2 value, which is off by about 0.6 eV. The conflicting VDE predictions by the MP2 and B3LYP methods for the $CO_2^-(H_2O)_m$, $m=0-5$ cluster anions are summarized in Table I. We leave these results without further comment, noting only that similar discrepancies between MP2 and B3LYP (mostly not in MP2's favor) were described previously in the case of OCS.[31]

At the levels of theory employed, the *ab initio* anion and neutral potential energy curves in the top panel of Fig. 5 intersect at 146.6°, 152.2°, 154.7°, and 157.5° for $m=0$, 1, 2, and 3, respectively. These intersection points lie 87, 319, 441, and 626 meV above the respective anion minima. Using B3LYP, the intersections are observed at 154.0°, 162.5°, 169.4°, and 172.0°, for $m=0$, 1, 2 and 3, respectively, lying 136, 374, 550, and 644 meV above the anion minima, respectively. Since all molecular degrees of freedom, with the exception of ∠OCO, were relaxed in the calculations, the

TABLE I. Vertical detachment energies (VDEs) of $CO_2^-(H_2O)_m$, $m=0-5$ calculated as described in the text using the MP2 and B3LYP methods with the aug-cc-pVTZ basis set, compared to the experimentally determined values.

	VDE (eV)		
m	MP2	B3LYP	Expt.
0	0.77	1.19	1.4[a]
1	1.65	2.06	1.96[b]
2	2.17	2.61	2.44[b]
3	2.60	2.97	2.85[b]
4	2.91	3.28	3.21[b]
5	3.18	3.62	3.46[b]

[a]Reference 47.
[b]Reference 24.

anion and neutral energies determined for a given OCO angle correspond to different anion and neutral geometries. Therefore, the above energy values are only crude lower bounds for the autodetachment barrier heights, as estimated at the levels of theory employed. Nonetheless, these results reveal the dual effect of stepwise hydration: (1) the stabilization of the anion equilibrium relative to the neutral potential minimum, and (2) the increase in the autodetachment barrier height. Both of these factors contribute to the increased stability of hydrated CO_2^-.

The above computational approach does not do justice to the complexity of the problem, because it fails to account for the effect of very diffuse, nearly-free-electron states on the anion. These states are particularly important in the proximity of the neutral states. As a case in point, the electron scattering on CO_2 revealed vibrational structures in the 0.4–0.9 eV range, well below the $^2\Pi_u$ resonance.[11] These structures cannot be accounted for without considering the low-lying diffuse electron states. These states are not considered properly in the above calculations due to basis-set limitations.

We therefore turn to the results from other workers using highly correlated *ab initio* methods with extended basis sets, which are, unfortunately, limited to bare CO_2^- only. Sommerfeld *et al.* showed that upon increasing the OCO angle starting from the bent CO_2^- equilibrium structure, the anion potential energy surface exhibits an about 57 meV barrier[48] and then drops below the bent equilibrium energy *before* crossing with the neutral surface.[35] Hence, the contribution of the very diffuse electron states lowers the energy of the adiabatically ground state of CO_2^-, particularly near the linear geometry. The crossing of the anion and neutral potential energy surfaces is also lowered in energy. The autodetachment barrier height estimated by Sommerfeld *et al.* is indeed significantly lower than thought previously:[34] 60 meV compared to the 87 meV "lower bound" estimated using the above MP2/aug-cc-pVTZ calculations for the $m=0$ case. Therefore, regarding the corresponding 87, 319, 441, and 626 meV values for $CO_2^-(H_2O)_m$, $m=0$, 1, 2, and 3, respectively, we conclude that while they reflect a correct trend of increasing stability of the hydrated cluster anions, they, in fact, *overestimate* the autodetachment barrier height.

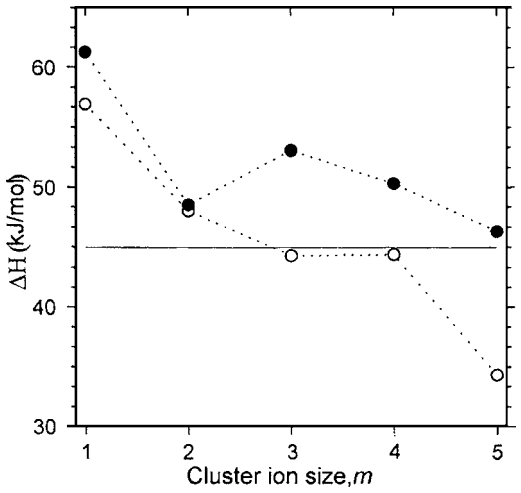

FIG. 6. Calculated enthalpy of evaporation (ΔH) as a function of $CO_2^-(H_2O)_m$ cluster size. The open and solid circles represent the values obtained using the B3LYP/6-311++G($3df$,$3pd$) and MP2/6-311++G($3df$,$3pd$) methods, respectively. The solid horizontal line indicates the asymptotic limit of $\Delta H(m)$ determined in the present experiments.

B. Water binding energy

The enthalpy of evaporation of a water molecule from $CO_2^-(H_2O)_m$, $\Delta H(m)$, can be determined from the energy balance of the following reaction:

$$CO_2^-(H_2O)_m \rightarrow CO_2^-(H_2O)_{m-l} + H_2O, \quad \Delta H(m). \tag{3}$$

From the data in Fig. 4, the asymptotic limit of $\Delta H(m)$ is 45.0 kJ/mol (for $m \geqslant 20$). However, $\Delta H(m)$ is expected to deviate significantly from the asymptotic limit as m decreases, generally corresponding to larger values for smaller clusters.

From the B3LYP/6-311++G($3df$,$3pd$) calculations, Balaj *et al.* estimated the dissociation enthalpy of $CO_2^-(H_2O)_m$, $m=0-5$ at 1 atm and 298 K.[25] Their results are plotted in Fig. 6 (open circles), with the horizontal line indicating the asymptotic limit of $\Delta H(m)$ derived from the present experiments. Despite the different pressure-temperature conditions, one should expect the size-dependent theoretical values to approach the experimental asymptotic limit from above, as m increases. As this is not what is seen in Fig. 6, we conclude that density-functional theory underestimates the hydration energetics.

For comparison, after optimizing the $CO_2^-(H_2O)_m$, $m=0-5$ cluster structures at the MP2/6-311++G** level (giving the same geometries as in Ref. 25, except for $m=5$, for which a more stable structure was found[18]), we calculated single-point MP2 energies with the 6-311++G($3df$,$3pd$) basis set. The corresponding $\Delta H(m)$ values are plotted in Fig. 6 (solid circles). The MP2 predictions are clearly in better agreement with the experiment than the B3LYP results of Balaj *et al.* Combining this observation with the adiabatic electron affinity and VDE calculations in Sec. IV A, we infer that B3LYP accounts fairly well for the electron binding energy, but not the water binding energy. For the latter, MP2 seems to do a better job.

The experimentally estimated asymptotic limit of $\Delta H \rightarrow 45.0$ kJ/mol for large m is very close to the heat of evapo-

ration of bulk water at 25 °C, 43.98 kJ/mol (0.456 eV/molecule).[49] This implies that in large $CO_2^-(H_2O)_m$ clusters ($m>20$), the outermost water molecules interact predominantly with the water network rather than the anionic core of the cluster.

C. Dissociation mechanism

The first two absorption bands of CO_2^- trapped in crystalline sodium formate were observed at 340 and 250 nm and assigned to the $^2B_1 \leftarrow X\,^2A_1$ and $^2A_1 \leftarrow X\,^2A_1$ electronic transitions, respectively.[50] The former transition was also seen at 365 nm, under a different procedure of crystal preparation.[51] The 250 nm transition was also observed in aqueous solution.[6,7] The photofragmentation at 355 nm has been suggested to involve the $^2B_1 \leftarrow X\,^2A_1$ transition.[26] The 266 nm wavelength used in the present work is closer to the second, $^2A_1 \leftarrow X\,^2A_1$ band, leading us to believe that the $CO_2^-(H_2O)_m$ cluster fragmentation at 355 and 266 nm may proceed via different excited electronic states of hydrated CO_2^-.

No detailed theoretical work is available in the literature for the excited-state potential energy surfaces of CO_2^- relevant to 266 nm photodissociation. As early as 1970, Claydon *et al.*[52] used semiempirical (INDO) methods to calculate the potential energy curves of CO_2^-. Other theoretical studies on CO_2^- targeted mainly the ground $X\,^2A_1$ and first excited $^2B_1$ states.[35,48,53–58] Therefore, we opted to examine the excited electronic states of CO_2^- using the configuration-interaction method with single excitations (CIS). The calculations are carried out for both the isolated and hydrated anion, $CO_2^-(H_2O)_m$, with $m=0$, 1, and 2. Many of the relevant anionic states are autodetaching in nature and the basis set used (6-31+G*) is admittedly rather small, which may lead one to believe that these calculations are of questionable value. However, the experimental results presented in this work highlight the dynamics occurring on these very states, indicating that in the presence of water molecules the autodetachment is suppressed sufficiently to allow anionic nuclear rearrangements. Ideally, it would be desirable to consider the electronic structure of larger $CO_2^-(H_2O)_m$ clusters, where the hydration stabilization pulls the excited states out of the autodetachment continuum into the realm of stable anionic states, but such calculations are prohibitively expensive. Hence, although computational difficulties prevented extending this work to larger clusters, it is assumed that the main qualitative features of the electronic structure, dissociation mechanism, and hydration effects can be understood on the basis of the available results.

In carrying out the calculations, all molecular and cluster geometries were constrained to C_s symmetry under which the irreducible representations of the C_{2v} point group transform as A_1, $B_2 \rightarrow A'$; A_2, $B_1 \rightarrow A''$. The constrained $CO_2^-(H_2O)_m$, $m=0-2$ geometries were optimized at either fixed OCO bending angles or fixed OC–O bond distances. The results of these potential energy scans for the low-lying electronic states of $CO_2^-(H_2O)_m$, $m=0-2$ are shown in Fig. 7. Although the calculations overestimate the excitation energies, as apparent from comparison of the vertical transition energies in Fig. 7 and the experimentally known absorption bands,[6,7,50,51] they do provide a semiquantitative guide to the electronic structure and photochemistry of hydrated CO_2^-.

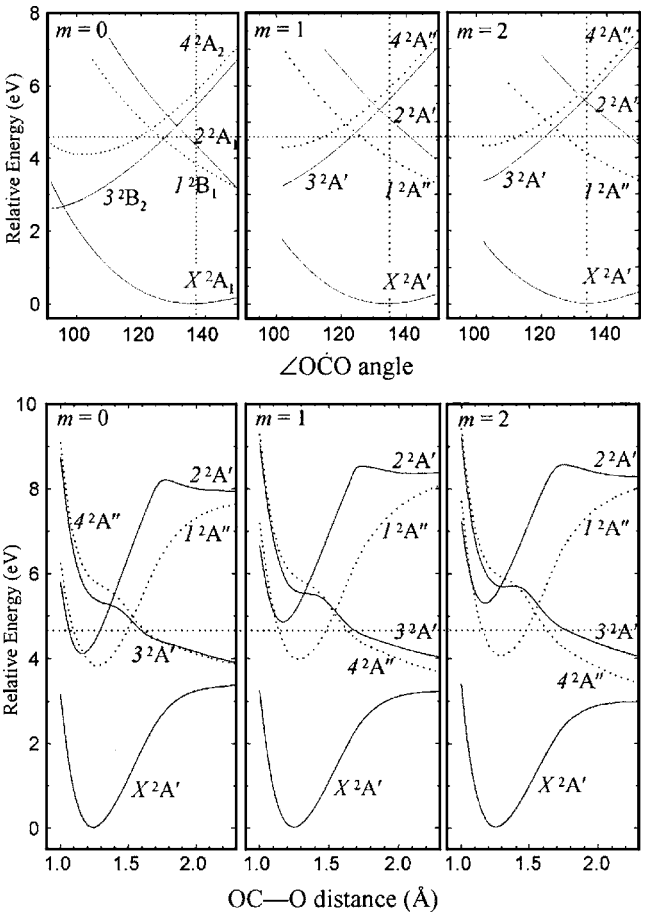

FIG. 7. Potential energy curves for $CO_2^-(H_2O)_m$, $m=0$, 1, and 2 as functions of the OCO bending angle (top) and the OC–O bond length (bottom). The horizontal dotted lines indicate the 266 nm photon energy, 4.661 eV. The vertical dotted lines in the top panels indicate the equilibrium OCO angle, 135°.

In addition to the electronic wave function symmetry, each state in Fig. 7 is assigned an *italics* label reflecting the energetic state ordering at the equilibrium geometry of bare CO_2^-. While the order of states may change with geometry and hydration, the italicized labels uniquely identify the relevant electronic states throughout the following discussion. For example, the $3\,^2B_2$ state, which is the third excited state at the CO_2^- equilibrium geometry, is found below the $X\,^2A_1$ state for bending angles less than ~101°, as seen in the top panel of Fig. 6 ($m=0$). This change in the $^2B_2$ and $^2A_1$ state ordering is similar to that in the isoelectronic NO_2.[59–62] (No attempt was made to explore the $X\,^2A_1$ and $3\,^2B_2$ state crossing regions in the presence of water molecules.)

Referring to Table I and Fig. 7, the excited anionic states for small m lie above the neutral ground state, i.e., these states belong to the autodetachment continuum. However, although electron detachment is the dominant photodestruction channel, anionic photodissociation is observed for parent clusters as small as $m=2$ (see Fig. 2). Increasing m suppresses the direct photodetachment, while the autodetachment via the excited anionic states discussed above becomes more important, as reflected in the loss of the

anisotropy of the photoelectron images with increasing m.[18] As m increases further, anionic dissociation becomes the dominant channel.

The dissociation of hydrated CO_2^- at 355 nm yielding O^- based fragments was proposed to result from the glancing intersection due to the Renner-Teller interaction of the $X\,^2A_1(^2A')$ and $1\,^2B_1(^2A'')$ electronic states at the linear CO_2^- geometry.[26] In view of the present results, the 355 nm dissociation dynamics can be described in more detail as follows. The core anion is promoted to the $1\,^2B_1(^2A'')$ excited state, which itself does not correlate to the O^-+CO dissociation limit (see Fig. 7, lower panel). However, the potential gradient in the Franck-Condon region of the $1\,^2B_1$ state directs the ion towards the linear geometry with equal O–C–O bond lengths (Fig. 7, top). Near the linearity, the 1 state couples with X state, followed by the OC–O^- bond dissociation of the latter.

Examining the computational results in Fig. 7, we note that the $CO_2^- \rightarrow O^-$+CO dissociation following the excitation to the $1\,^2B_1$ state could also proceed, in principle, via the genuine conical intersection between the 1 and 4 states, both of which are of the same $^2A''$ electronic symmetry for C_s geometries, but of different, $^2B_1$ and $^2A_2$ symmetries in C_{2v}. The potential energy curves corresponding to these states are indicated in Fig. 7 by dotted lines. As seen in the lower panel of the figure, the 4 state does indeed correlate to the O^-+CO dissociation limit. However, the intersection with the 1 state lies in the energy range not accessible at 355 nm.

At 266 nm, the $2\,^2A_1 \leftarrow X\,^2A_1$ transition in CO_2^- is believed to be excited. As noted above, the CIS results in Fig. 7 generally overestimate the excitation energies, but we confirmed that the vertical $2\,^2A_1(^2A') \leftarrow X\,^2A_1(A')$ transition is indeed accessible at 266 nm in both bare and hydrated ($m=1,2$) anion using higher-level complete active space self-consistent-field and symmetry adapted cluster/configuration interaction (SAC-CI) calculations. The potential energy curves relevant to 266 nm excitation are shown in Fig. 7 by solid lines.

The initially prepared 2 state or the core anion does not correlate with the O^-+CO dissociation limit. However, it intersects (conically) with the dissociative $3\,^2B_2(^2A')$ state. The crossing occurs at a bent geometry (about 135°), in contrast to the linear Renner-Teller crossing between the X and 1 states believed responsible for the 355 nm process.[26] Therefore, 266 nm dissociation does not have to involve the linear region of the coordinate space, where metastable CO_2^- is most subject to the autodetachment decay. This conclusion may imply that despite the higher photon energy, the 266 nm mechanism is less dependent on the solvent stabilization, compared to 355 nm. Thus, the observed decrease (with increasing m) of the 266 nm dissociation yield, relative to that at 355 nm, may, in fact, be due to the sharp increase (with m) in the 355 nm dissociation, while the 266 nm yield is possibly less affected by the cluster size.

For $m=2$, the oscillator strengths of the $1\,^2A'' \leftarrow X\,^2A'$ and $2\,^2A' \leftarrow X\,^2A'$ transitions, as estimated using the CIS calculations, are 0.0093 and 0.0223, respectively. These values are consistent with the relative 266 and 355 nm dissociation cross sections observed in this work.

D. Dissociation energy of hydrated CO_2^-

As seen in Fig. 4, in the large-m limit of the core-dissociation channel, the average number of water molecules evaporated at 266 nm (4.66 eV) exceeds that at 355 nm (3.49 eV) by 2.2. This compares to the average difference of 2.5 molecules expected under the assumption that the evaporation of one H_2O requires 0.466 eV (see Sec. III). This fairly close agreement confirms that the energetics are approximately accounted for and the core-dissociation pathways at both wavelengths yield fragments in the same electronic states.

In the 266 nm core-dissociation channel, the average number of evaporated water molecules is $\langle k\rangle=4.66$ for $m \geqslant 20$. Given the estimated 0.466 eV evaporation energy per molecule, approximately 4.66×0.466 eV$=2.17$ eV of the 266 nm photon energy is spent on water evaporation and only the remaining 2.49 eV, at the most, is used to dissociate the OC–O bond. This estimate is meaningful only if the energetics of the following two reactions in large clusters are comparable:

$$CO_2^-(H_2O)_m \rightarrow CO_2^-(H_2O)_{m-1} + H_2O, \quad \Delta H(m), \tag{4a}$$

$$O^-(H_2O)_m \rightarrow O^-(H_2O)_{m-1} + H_2O, \quad \Delta H'(m). \tag{4b}$$

Using MP2/aug-cc-pVTZ calculations at 298 K and 1 atm, $\Delta H'(m)$ was estimated as 1.076, 0.791, 0.662, and 0.478 eV for $m=0$, 1, 2, 3, and 4, respectively, including the zero-point energy corrections. Given the $\Delta H(m)$ values calculated in Sec. IV B, the difference between the water binding energies for the O^- and CO_2^- based clusters can be estimated as $\Delta H'-\Delta H=0.476$, 0.299, 0.180, −0.029, and 0.003 for $m=0$, 1, 2, 3, 4, and 5, respectively. Similar trend can be obtained by combining the results of the density-functional calculations by Balaj *et al.*[25] on $CO_2^-(H_2O)_m$ and by Seta *et al.*[63] on $O^-(H_2O)_m$. Hence the difference between $\Delta H'$ and ΔH becomes small in the limit of large m. Therefore, the above estimate for the energy required to break the OC–O bond in large $CO_2^-(H_2O)_m$ clusters, 2.49 eV, is reasonable. This value compares to the 3.46 eV bond dissociation energy of bare CO_2^-.

V. SUMMARY

The photofragmentation of the mass-selected $CO_2^-(H_2O)_m$, $m=2-40$ cluster anions proceeds via two types of pathways: the core-dissociation channel resulting in the formation of $O^-(H_2O)_{m-k}$, and the solvent-evaporation channel, which is manifest in the loss of several water molecules from the parent cluster. The average number of water molecules lost in the fragmentation process, $\langle k\rangle$, varies between 0.5 and 4.7 in the core-dissociation channel and between 7.0 and 10.0 in the solvent-evaporation channel. From the asymptotic value of $\langle k\rangle$, the enthalpy of H_2O evaporation from the cluster is determined as 0.466 ± 0.001 eV, compared to the heat of evaporation of bulk water, 0.456 eV at 25 °C. The C–O bond dissociation energy of the CO_2^- core in the $CO_2^-(H_2O)_m$, $m \geqslant 20$ cluster anions is estimated as 2.49 eV, compared to 3.46 eV for bare CO_2^-. *Ab initio* and density-functional calculations illuminate the twofold effect of step-

wise hydration: (1) the stabilization of the anion equilibrium relative to the neutral potential minimum, and (2) the increase in the autodetachment barrier height.

Although 355 and 266 nm excitations produce the same types of anionic fragments, different electronic transitions and dissociation mechanisms are implicated in the two excitation regimes. The 355 nm excitation involves the $1\,^2B_1 \leftarrow X\,^2A_1$ electronic transition at the bent CO_2^- geometry. The two states are coupled at linear geometry by the Renner-Teller interaction and the $CO_2^- \rightarrow O^- + CO$ dissociation is believed to proceed via the ground electronic state. In contrast, the 266 nm dissociation is initiated by $2\,^2A_1 \leftarrow X\,^2A_1$ electronic transition. Although the excited $2\,^2A_1$ does not itself correlate with the $O^- + CO$ dissociation limit, the dissociation can proceed via a conical intersection with the $3\,^2B_2(^2A')$ state.

ACKNOWLEDGMENTS

The authors would like to acknowledge stimulating discussions with Professor Ludwik Adamowicz concerning the computational aspects of this project. This work is supported by NSF Grant No. CHE-0134631.

[1] F. L. Arnot and C. Beckett, Proc. R. Soc. London, Ser. A **168**, 103 (1938).
[2] G. A. Ropp and C. E. Melton, J. Am. Chem. Soc. **80**, 3509 (1958).
[3] D. W. Ovenall and D. H. Whiffen, Mol. Phys. **4**, 135 (1961).
[4] J. H. Lunsford and J. P. Jayne, J. Phys. Chem. **69**, 2182 (1965).
[5] J. F. Paulson, J. Chem. Phys. **52**, 963 (1970).
[6] J. P. Keene, Y. Raef, and A. J. Swallow, in *Pulse Radiolysis*, edited by M. Emert, J. P. Keene, and A. J. Swallow (Academic, London, 1965), p. 99.
[7] P. Neta, M. Simic, and E. Hayon, J. Phys. Chem. **73**, 4207 (1969).
[8] C. D. Cooper and R. N. Compton, Chem. Phys. Lipids **14**, 29 (1972).
[9] G. J. Schulz, Phys. Rev. **128**, 178 (1962).
[10] M. J. W. Boness and G. J. Schulz, Phys. Rev. A **9**, 1969 (1974).
[11] M. Allan, J. Phys. B **35**, L387 (2002).
[12] R. N. Compton, P. W. Reinhardt, and C. D. Cooper, J. Chem. Phys. **63**, 3821 (1975).
[13] C. E. Klots and R. N. Compton, J. Chem. Phys. **67**, 1779 (1977).
[14] C. E. Klots, J. Chem. Phys. **71**, 4172 (1979).
[15] M. J. DeLuca, B. Niu, and M. A. Johnson, J. Chem. Phys. **88**, 5857 (1988).
[16] R. Mabbs, E. Surber, L. Velarde, and A. Sanov, J. Chem. Phys. **120**, 5148 (2004).
[17] T. Tsukuda, M. A. Johnson, and T. Nagata, Chem. Phys. Lett. **268**, 429 (1997).
[18] E. Surber, R. Mabbs, T. Habteyes, and A. Sanov, J. Phys. Chem. A **109**, 4452 (2005).
[19] M. Armbruster, H. Haberland, and H. G. Schindler, Phys. Rev. Lett. **47**, 323 (1981).
[20] H. Haberland, C. Ludewigt, H. G. Schindler, and D. R. Worsnop, J. Chem. Phys. **81**, 3742 (1984).
[21] H. Haberland, H. Langosch, H. G. Schindler, and D. R. Worsnop, J. Phys. Chem. **88**, 3903 (1984).
[22] J. V. Coe, G. H. Lee, J. G. Eaton, S. T. Arnold, H. W. Sarkas, K. H. Bowen, C. Ludewigt, H. Haberland, and D. R. Worsnop, J. Chem. Phys. **92**, 3980 (1990).
[23] A. W. Castleman and K. H. Bowen, J. Phys. Chem. **100**, 12911 (1996).
[24] T. Tsukuda and T. Nagata, J. Phys. Chem. A **107**, 8476 (2003).
[25] O. P. Balaj, C. K. Siu, I. Balteanu, M. K. Beyer, and V. E. Bondybey, Chem.-Eur. J. **10**, 4822 (2004).
[26] T. Habteyes, L. Velarde, and A. Sanov, Chem. Phys. Lett. **424**, 268 (2006).
[27] L. Velarde, T. Habteyes, and A. Sanov, J. Chem. Phys. **125**, 114303 (2006).
[28] M. A. Johnson and W. C. Lineberger, in *Techniques for the Study of Ion Molecule Reactions*, edited by J. M. Farrar and W. H. Saunders (Wiley, New York, 1988), p. 591.
[29] A. T. J. B. Eppink and D. H. Parker, Rev. Sci. Instrum. **68**, 3477 (1997).
[30] D. W. Chandler and P. L. Houston, J. Chem. Phys. **87**, 1445 (1987).
[31] E. Surber, S. P. Ananthavel, and A. Sanov, J. Chem. Phys. **116**, 1920 (2002).
[32] M. L. Alexander, N. E. Levinger, M. A. Johnson, D. Ray, and W. C. Lineberger, J. Chem. Phys. **88**, 6200 (1988).
[33] L. Velarde, T. Habteyes, and A. Sanov, J. Chem. Phys. **125**, 114303 (2006).
[34] G. L. Gutsev, R. J. Bartlett, and R. N. Compton, J. Chem. Phys. **108**, 6756 (1998).
[35] T. Sommerfeld, J. Phys. B **36**, L127 (2003).
[36] M. J. Frisch, G. W. Trucks, H. B. Schlegel *et al.*, GAUSSIAN 03 Gaussian Inc., Wallingford, CT, 2004.
[37] L. Fredin, B. Nelander, and G. Ribbegard, Chem. Scr. **7**, 11 (1975).
[38] M. Falk and A. G. Miller, Vib. Spectrosc. **4**, 105 (1992).
[39] A. Schriver, L. Schriver-Mazzuoli, P. Chaquin, and E. Dumont, J. Phys. Chem. A **110**, 51 (2006).
[40] K. I. Peterson and W. Klemperer, J. Chem. Phys. **80**, 2439 (1984).
[41] K. I. Peterson, R. D. Suenram, and F. J. Lovas, J. Chem. Phys. **94**, 106 (1991).
[42] T. L. Tso and E. K. C. Lee, J. Phys. Chem. **89**, 1612 (1985).
[43] B. Jonsson, G. Karlstrom, and H. Wennerstrom, Chem. Phys. Lett. **30**, 58 (1975).
[44] P. A. Block, M. D. Marshall, L. G. Pedersen, and R. E. Miller, J. Chem. Phys. **96**, 7321 (1992).
[45] J. Sadlej, J. Makarewicz, and G. Chalasinski, J. Chem. Phys. **109**, 3919 (1998).
[46] J. Makarewicz, T. K. Ha, and A. Bauder, J. Chem. Phys. **99**, 3694 (1993).
[47] K. H. Bowen and J. G. Eaton, in *The Structure of Small Molecules and Ions*, edited by R. Naaman and Z. Vager (Plenum, New York, 1988), p. 147.
[48] T. Sommerfeld, H. D. Meyer, and L. S. Cederbaum, Phys. Chem. Chem. Phys. **6**, 42 (2004).
[49] *CRC Handbook of Chemistry and Physics*, 84th ed., edited by D. R. Lide (CRC, Boca Raton, FL, 2004).
[50] G. W. Chantry and D. H. Whiffen, Mol. Phys. **5**, 189 (1962).
[51] K. O. Hartman and I. C. Hisatsune, J. Chem. Phys. **44**, 1913 (1966).
[52] C. R. Claydon, G. A. Segal, and H. S. Taylor, J. Chem. Phys. **52**, 3387 (1970).
[53] M. Krauss and D. Neumann, Chem. Phys. Lipids **14**, 26 (1972).
[54] J. Pacansky, U. Wahlgren, and P. S. Bagus, J. Chem. Phys. **62**, 2740 (1975).
[55] D. G. Hopper, Chem. Phys. **53**, 85 (1980).
[56] W. B. England, Chem. Phys. Lett. **78**, 607 (1981).
[57] T. N. Rescigno, W. A. Isaacs, A. E. Orel, H. D. Meyer, and C. W. McCurdy, Phys. Rev. A **65**, 032716 (2002).
[58] C. W. McCurdy, W. A. Isaacs, H. D. Meyer, and T. N. Rescigno, Phys. Rev. A **67**, 042708 (2003).
[59] G. D. Gillispie and A. U. Khan, J. Chem. Phys. **65**, 1624 (1976).
[60] V. Kurkal, P. Fleurat-Lessard, and R. Schinke, J. Chem. Phys. **119**, 1489 (2003).
[61] C. F. Jackels and E. R. Davidson, J. Chem. Phys. **65**, 2941 (1976).
[62] C. P. Blahous, B. F. Yates, Y. M. Xie, and H. F. Schaefer, J. Chem. Phys. **93**, 8105 (1990).
[63] T. Seta, M. Yamamoto, M. Nishioka, and M. Sadakata, J. Phys. Chem. A **107**, 962 (2003).